Mon. Not. R. Astron. Soc. **000**, 1–?? (2001) Printed 12 November 2018 (MN LATEX style file v2.2)

X-ray reflection in the Seyfert galaxy 1H 0419-577 revealing strong relativistic effects in the vicinity of a Kerr black hole

A. C. Fabian[1⋆], G. Miniutti[1], K. Iwasawa[1] and R.R. Ross[2]
[1]*Institute of Astronomy, Madingley Road, Cambridge CB3 0HA*
[2]*Physics Department, College of the Holy Cross, Worcester, MA 01610, USA*

12 November 2018

ABSTRACT

We report results obtained from six XMM–Newton observations of the Seyfert galaxy 1H 0419–577. The source was observed in a wide range of different flux levels, allowing its long–term spectral variability to be studied in detail as already reported by Pounds et al (2004a; 2004b). Here we show that the X–ray spectrum is well described by a simple two–component model comprising a power law with constant spectral shape and variable normalisation and a much more constant ionised reflection component from the inner accretion disc which carries the signature of strong relativistic effects. One of the observations was performed when the source was in a particularly low flux state in which the X–ray spectrum is rather peculiar and exhibits a very flat hard spectrum (with spectral index close to 1 in the 2–10 keV band) with broad residuals below 6.6 keV (rest–frame) and a steep soft excess below about 1 keV. We interpret the spectrum as being reflection–dominated by X–ray reprocessed emission from the inner accretion disc. The primary continuum, which illuminates the disc, is almost completely unobserved possibly because of strong light bending towards the central super–massive black hole. The ionised reflection model simultaneously accounts for the broad hard residuals and hard flat spectrum and for the soft excess. The same model provides an excellent description of the data at all the other flux levels, the most important difference being a variation in the power law normalisation. Our spectral decomposition and interpretation of the spectral variability implies that most of the X–ray emission in this source originates from within few gravitational radii from the central black hole and requires that the compact object is almost maximally spinning.

Key words: line: formation – galaxies: active – X-rays: galaxies – X-rays: general – galaxies: individual: 1H 0419–577

1 INTRODUCTION

1H 0419–577 is an EUV-luminous, radio-quiet, optically broad-line, Seyfert 1–1.5 galaxy at redshift $z = 0.104$ (Pye et al 1995; Marshall, Fruscione & Carone 1995). Its 2–10 keV luminosity of 5×10^{44} erg s^{-1}(Guainazzi et al 1998; Page et al 2002) puts it around the Seyfert–quasar borderline. It shows remarkable long-term soft X-ray variability ranging from a very steep to a relatively flat spectrum (Guainazzi et al 1998; Turner et al 1999; Page et al 2002).

The source has been observed several times with XMM-Newton, and previous analysis by Pounds et al (2004a; 2004b) revealed that the dominant spectral variability is due to a steep power-law component. 1H 0419–577 has a high state dominated by this power law, of photon index $\Gamma \simeq 1.8$, and a low state where the spectrum is unusually very flat, $\Gamma \sim 1$ in the 2–10 keV band. Pounds et al obtain good fits to the low-state spectrum with either a very broad iron-K line and continuum reflection or partial covering. A strong blackbody component was also included to model a prominent soft excess below about 1 keV. For the reflection fit, a very high reflection factor, $R \sim 3.5$, was required and the irradiating power-law is still very flat $\Gamma \sim 1.26$). Guainazzi et al (1998) found what they considered to be an improbably high reflection fraction ($R \sim 10$) from their spectral fitting of BeppoSAX data. ASCA data revealed for the first time the presence of a Fe line in 1H 0419–577 (Turner et al 1999).

The possibility of a reflection–dominated spectrum in the low flux state of 1H 0419–577 matches very well the predictions of a light-bending model we recently developed for the strong gravity regime in the well-studied Seyfert galaxy MCG–6-30-15 (Fabian & Vaughan 2003; Miniutti et al 2003; Miniutti & Fabian 2004; Vaughan & Fabian 2004) and for the very high state of the Galactic black hole Candidate XTE J1650–500 (Miniutti, Fabian & Miller 2004; Rossi et al. 2005). This model consists of power–law (PLC) and reflection-dominated (RDC) components and was able also to explain the complex spactrum and variability of the NLS1 1H 0707-

⋆ acf@ast.cam.ac.uk

495 (Fabian et al. 2002; 2004). The PLC is assumed to originate in a compact region at a few gravitational radii ($r_{\rm g} = GM/c^2$) above the innermost disc. The emitting region can be either static or comoving with the accretion flow, point–like or ring–like, withouth much differences in the resulting behaviour. In Miniutti & Fabian (2004) we assumed the PLC originates from a ring–like structure at $2\,r_g$ from a Kerr black hole axis, but similar results are obtained for compact sources within about $4\,r_g$ and even for a primary source on the rotation axis of the black hole (such as in the lamp–post model, see e.g. Martocchia, Karas & Matt 2000).

The ring–like configuration is not necessarily the actual emitting structure we have in mind at any given time, but the time–averaged configuration over the timescale needed to extract good quality spectra from present X–ray observatories. A collection of static/corotating sources related e.g. to magnetic dissipation processes preferentially occurring at few r_g from the hole in a patchy corona, X–ray emission in the base of a compact jet (e.g. Markoff, Falcke & Fender 2001), or due to internal shocks from aborted jets close to the hole axis (Ghisellini, Harrdt, Matt 2004) might all be viable physical mechanisms, the list being far from exhaustive.

We note here that evidence for an orbiting reflecting spot, possibly related to a corotating illuminating flare above it (one of the primary sources?) at about $10\,r_g$ from the black hole in NGC 3516 has been reported recently (Iwasawa, Miniutti & Fabian 2004). Flares/emitting regions located even closer to the central mass, would prove difficult to follow in reflection with current detectors, especially if lasting, as it is likely due to turbulence and shear in the innermost flow, less than one orbital period. A reasonable zeroth–order approximation for the time–averaged emitting source geometry seems that of assuming a ring representing globally the region of preferential energy dissipation since the natural symmetry is around the black hole axis.

The main idea of the light bending model is that, since the primary source is in a region of strong gravity, the flux of the observed PLC is reduced by gravitational light bending which focus radiation down onto the disc where the RDC originates (the closer the source to the black hole, the stronger the effect). The PLC can then appear to vary in amplitude by a large factor (an order of magnitude or more) as the location of the primary source is allowed to vary, even its intrinsic luminosity is constant, while the RDC changes only little. The spectrum of the RDC is affected by the redshifts expected from a component situated only a few $r_{\rm g}$ from a black hole. The main prediction of this model is that the spectrum becomes more and more reflection–dominated as the PLC flux drops.

Here we apply the light-bending model to the XMM-Newton data of 1H 0419–577. We use new ionised slab models for the reflection component (Ross & Fabian 2005) based on previous calculations by Ross et al (1993; 1999; 2002), the whole spectrum of which is blurred relativistically to include the effects of emission originating in a geometrically thin accretion disc around a rotating black hole. Our aim is to see whether a simple two-component (PLC plus RDC) light-bending model explains the whole broadband spectrum of 1H 0419–577 and its variability.

2 THE XMM–NEWTON OBSERVATIONS

XMM–Newton observed 1H 0419–577 six times between December 2000 and September 2003 (orbits 181, 512, 558, 605, 649, and 690). The data have been kindly provided to us by K.A. Pounds (see Pounds et al 2004b for details on data reduction) except for orbit 181 whose data have been downloaded from the XMM–Newton Science Archive. We only make use here of the EPIC–pn spectra which were grouped to a minimum of 20 counts per energy bin to allow the use of the χ^2 minimisation during spectral fitting. Errors are quoted at the 90 per cent confidence level for one interesting parameter.

3 THE LOW FLUX STATE OF 1H 0419–577: XMM–NEWTON ORBIT 512

As reported by Pounds et al (2004a) one of the XMM–Newton observations (orbit 512) caught 1H 0419–577 in a low flux state. Low flux states are of great interest in the framework of the light bending model because they are predicted to be dominated by strong disc reflection from the accretion disc. This is because low flux states correspond to geometries in which the primary X–ray source is very close to the black hole, so that most of its emission is bent onto the accretion disc, reducing the continuum flux that reaches the observer at infinity directly while at the same time enhancing the disc illumination, and therefore the reflection fraction (Miniutti & Fabian 2004).

When a simple power–law model is fitted to the data in the 2–10 keV band, a very flat photon index ($\Gamma \sim 1$) is obtained leaving clear broad residuals below about 6 keV in the observer frame, corresponding to about 6.6 keV in the rest–frame. Re–inserting the 0.5–2 keV data reveals a strong soft excess below about 1 keV. The residuals (in terms of σ) of such a fit are shown in Fig. 1 where the soft excess and broad hard residuals are seen.

As reported by Pounds et al (2004a) the soft excess can be described by black body emission, while the broad hard residuals can be accounted for with a partial covering model by slightly ionised matter. In such a partial covering fit, narrow iron emission is also detected at $E = 6.21 \pm 0.11$ in the source rest–frame, barely consistent with the iron Kα energy ($\geqslant$ 6.4 keV). The observed redshifted energy is at odds with the partial covering interpretation given that the absorbing column should produce neutral or even slightly ionised iron emission. The iron line energy could still arise from the absorbing matter if the absorber originates in an outflow (but where is the blueshifted component?), in an inflow, or if it is located close to the black hole and suffers gravitational redshift. However, the absorption edge is not redshifted by the same amount as the line, but lies at 7.10 ± 0.06 keV in the source rest–frame giving rise to a somewhat inconsistent picture (though at the 90 per cent level only).

Pounds et al (2004a) also explored a different interpretation of the hard spectrum in terms of broad relativistic iron emission and strong reflection which gave a comparable good fit to the data as the partial covering model with a large line equivalent width of about 1 keV. The power–law photon index was still very flat as with the partial covering model, challenging Comptonisation models for the X–ray continuum production (Haardt & Maraschi 1991). However, the use of an inconsistent reflection model (relativistic line at 6.9 keV plus a neutral reflection continuum which is not relativistically blurred) might have affected the spectral results.

Here we apply a spectral decomposition inspired by the light bending model to the spectrum of the low flux state. We consider the 0.5–10 keV data, because of some residual calibration uncertainties in the EPIC–pn soft energy band (Kirsch et al 2004). The model comprises only two broadband components, namely a power-law, and an ionised reflection model where reflection continuum and emission lines are computed self–consistently (Ross & Fabian 2005). The reflection spectrum is the result of a power–

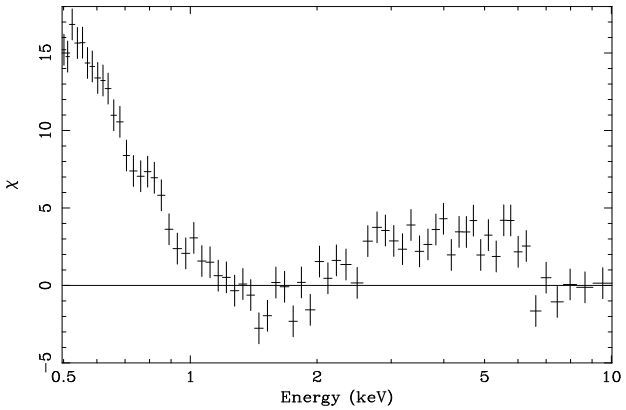

Figure 1. Ratio (in terms of σ) of the data of orbit 512 to a power law model fitted in the 2–10 keV band only. The figure shows the presence of a soft excess below about 1 keV and broad residuals between 3 and 6 keV (observer frame, $z = 0.104$).

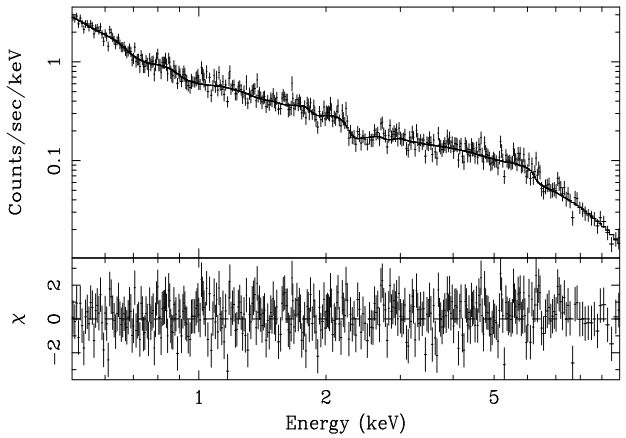

Figure 2. The 0.5-10 keV spectrum and residuals (in terms of σ) for the RDC plus PLC model of the LF state data (orbit 512), producing an excellent fit with $\chi^2 = 626$ for 638 degrees of freedom.

law illumination of Compton thick material, and we tied its photon index to that of the visible power–law component. The reflection model allows for variable iron abundance that was left as a free parameter of the model. The relativistic blurring makes use of the LAOR kernel describing relativistic effects on the spectral shape resulting from emission in an accretion disc orbiting a Kerr black hole (Laor 1991). The outer disc radius ($r_{\rm out}$) was fixed at its maximum possible value of $400\ r_g$, while the inner disc radius ($r_{\rm in}$) and disc inclination were allowed to vary. The emissivity profile, describing the dependency of the emissivity ϵ with the radial position on the disc, has the form of a broken power law with $\epsilon = r^{-q_{\rm in}}$ for $r_{\rm in} \leqslant r \leqslant r_{\rm br}$ and $\epsilon = r^{-q_{\rm out}}$ for $r_{\rm br} \leqslant r \leqslant r_{\rm out}$, where $r_{\rm br}$ is a break radius on the disc.

All spectral fits include photoelectric absorption fixed at the Galactic value ($N_{\rm H} = 2 \times 10^{20}$ cm^{-2}) and an additional absorption component at the redshift of 1H 0419–577 to account for possible excess absorption local to the source. Our aim is to explore whether the ionised reflection model can simultaneously account for the hard broad residuals, the flat spectrum, and the soft excess below 1 keV and to see whether a more consistent reflection model can remove the requirement for the implausibly flat 2–10 keV spectral shape.

With the addition of an absorption edge at ~ 0.74 keV, consistent with O VII in a warm absorber, our model provides a very good description of the low flux state data with $\chi^2 = 626$ for 638 degrees of freedom and null hypothesis probability of 0.636. No additional edge at 7.1 keV is required nor an absorption component above 2 keV. Both the soft excess and the hard spectrum are very well described by the relativistically blurred ionised reflection model. The 0.5–10 keV spectrum and best-fit residuals (in terms of σ) are shown in Fig. 2. The best–fit power law has a photon index of $\Gamma \simeq 2.2$, much steeper than previously derived (Pounds et al. 2004a) and totally consistent with standard Comptonisation models. As mentioned, this is most likely the effect of using a self–consistent reflection model in which emission lines and the reflection continuum are computed together and affected by the the same Doppler and gravitational shifts in the accretion disc.

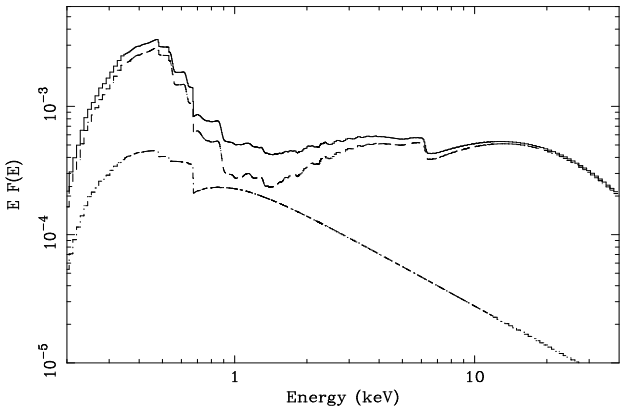

Figure 3. The best–fit model for the LF state of orbit 512 (see Fig. 2) is shown in the 0.2–40 keV band. The two spectral components are shown, with the RDC dominating both the soft and hard bands, with some PLC contamination in the intermediate band. The sum of the two spectral components, i.e. the total best–fit model, is also shown. The resulting reflection–dominated spectrum explains simultaneously both the flat spectral shape and broad residuals in the hard band and the soft excess below 1 keV.

In Fig. 3, we show the best–fit model in the (broader than fitted) energy range between 0.2 keV and 40 keV. From the Figure, the origin of the hard (2–10 keV) flat spectrum and steep soft excess below 1 keV is clear and due to the RDC. The spectrum is almost completely reflection–dominated with only little contribution from the power–law. This means that the reflection fraction (i.e. the relative amplitude of the RDC with respect to the PLC continuum) is much larger than unity and that the reflector is seeing much more illuminating flux than we detect at infinity as the PLC of the spectrum. This is expected if the primary PLC emission is strongly anisotropic and preferentially shining towards the disc. One possibility is provided by strong light bending which is effective if the primary PLC source is located only few r_g from the black hole producing low flux and reflection–dominated states. In this case, the RDC is emitted from the inner regions of the disc and is therefore strongly distorted by relativistic effects.

The parameters of the relativistic blurring support an interpretation in terms of strong relativistic effects. The emissivity profile ($\epsilon = r^{-q}$) is best described by a broken power–law with $q_{\rm in} = 7.0 \pm 0.7$ within the break radius $r_{\rm br} = 3.5^{+2.3}_{-0.7}\ r_g$ and $q_{\rm out} = 3.7 \pm 0.6$ at larger radii. The steep emissivity indicates that the disc is illuminated mostly in its very inner regions supporting the idea that the primary source is very close to the black hole. This is the region where light bending effects are most effective (and actually unavoidable) in reducing the PLC at infinity and therefore in producing a reflection–dominated spectrum. We also point out that

if this is the case, the emissivity profile would indeed result to be well approximated by a broken power law, much steeper in the inner disc and flatter in the outer regions (Martocchia, Karas & Matt 2000; Miniutti & Fabian 2004), as observed in this low flux state of 1H 0419–577.

The observer inclination is not very well constrained (being degenerate with the line energy or disc ionisation state) with a best–fit value of 36 ± 10 degrees. The best–fit inner disc radius is $1.4\ r_g$ with a 90 per cent upper limit at $2\ r_g$, very close to the innermost stable circular orbit around a maximally rotating Kerr black hole ($\sim 1.24\ r_g$), strongly suggesting that the black hole in 1H 0419–577 is rapidly rotating. The error on $r_{\rm in}$ is so small because emission from the innermost regions of the accretion disc is necessary to reproduce the broad curvature of the spectrum in the Fe K band.

The reflection model requires iron to be overabundant with respect to solar, the best–fit value being $(\ 3.8 \pm 1.5\ ) \times$ solar. Together with the large reflection fraction, this explains the large value of the equivalent width of the broad iron line (about 1 keV) obtained by Pounds et al (2004a) when fitting the hard residuals with a relativistic line profile. The high iron abundance we find is not unique to this object and is required e.g. in MCG–6-30-15 and 1H 0707-495 (Vaughan & Fabian 2004; Fabian et al 2002; 2004), also well described by a similar spectral model. We note that Shemmer et al (2004) recently found a metallicity–accretion rate correlation by studying a sample of active galaxies in the near–infrared (see the reference for possible interpretations). The mass of the black hole in 1H 0419–577 can be estimated by using the Kaspi et al (2000) relationship between Hβ line width, λL_λ (5100 Å) luminosity, and black hole mass. The optical measurements for 1H 0419–577 are reported in Grupe et al (2004) and we estimate a black hole mass of 1–2 $\times\ 10^8\ M_\odot$ (see also Pounds et al 2004b), which gives $L_{\rm Edd} = 1.3$–2.6×10^{46} erg s^{-1}. By considering the bolometric luminosity of 2.4×10^{46} erg s^{-1} (Grupe et al 2004), 1H 0419–577 might indeed be accreting at very high rate. It is therefore possible that MCG–6-30-15, 1H 0707-495, and 1H 0419–577 are all accreting at high rate and mainly differ by a different black hole mass, much higher in 1H 0419–577 as the lack of rapid large amplitude X–ray variability (as opposed to the other two sources) also indicates.

Finally, from the reflection model we measure an ionisation parameter of $\xi = 45 \pm 18$ erg cm s^{-1} for the reflector surface. However, since the radial dependency of the emissivity profile implies that the inner disc is much more illuminated than the outer regions, it is very likely that the ionisation structure on the disc surface is also strongly dependent on r. The most naive expectation (for a disc with approximately constant density) is that the disc is more ionised in the inner than outer regions, while we have used so far a reflection model with uniform ionisation parameter. We then replaced our simple reflection model by a composite one, in which the inner disc is allowed to have a different ionisation state than the outer one, with a break radius $r_{\rm br}$ where the ionisation parameter and the emissivity profile change abruptly. This is of course a zeroth–order approximation for a real situation in which the ionisation parameter is a function of r. We obtain a very good description of the data with $\chi^2 = 620$ for 637 degrees of freedom, which represents a modest but somewhat significant improvement on the single–reflector fit (98.7 per cent according to the F–test). The best–fit ionisation parameters are $\xi_{\rm in} = 69 \pm 20$ erg cm s^{-1} in the inner disc from $1.24\ r_g$ to $4.7\ r_g$, and $\xi_{\rm out} = 29 \pm 16$ erg cm s^{-1} out to $400\ r_g$. As in the previous fit, the emissivity profile is steeper in the inner disc and flatter in the outer. With this composite model, the 0.5–10 keV spectrum is completely reflection–dominated and only an upper limit on the PLC normalisation can be measured (see Table 2 for details).

XMM orbit	181	512	558	605	649	690
pn exposure	5.7	12.1	7.8	11.2	10.7	11.4
2–10 keV Flux	15.4	6.5	6.7	9.6	8.8	8.5
0.5–10 keV Flux	29.5	8.2	9.4	16.7	14.7	13.7
Flux state	HF	LF	LF	IF	IF	IF

Table 1. EPIC–pn net exposures (in ks), and 2–10 keV, 0.5-10 keV fluxes (in 10^{-12} erg s^{-1} cm^{-2}) for the six XMM–Newton observations of 1H 0419–577. Fluxes (absorbed) are obtained from the best–fit models described in Section 4.1 and Table 2. Based on the measured flux, we divide the observations into three groups, corresponding to low flux (LF), intermediate flux (IF), and high flux (HF) states.

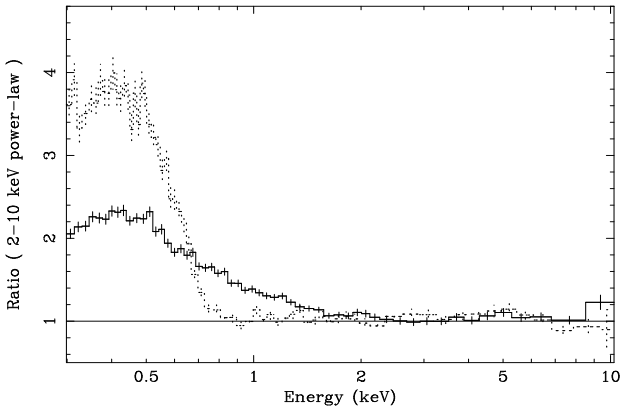

Figure 4. Ratio to a power law fitted in the 2–10 keV band for a LF state (orbit 558, dotted grey) and a HF state (orbit 181, solid black) observation. The 2-10 keV photon index is flat in the LF state ($\Gamma = 1.31$) and steeper in the HF ($\Gamma = 1.80$). The soft excess rises steep in the LF state, while is much more gradual in the HF state.

4 SPECTRAL VARIABILITY: THE REMAINING XMM–NEWTON OBSERVATIONS

Based on our best–fit model which will be discussed below, we were able to compute the fluxes for the six XMM–Newton observations which are reported in Table 1 together with the exposures obtained with the EPIC–pn camera after screening. Hereafter we define orbits 512 and 558 as low–flux (LF) states, orbits 605, 649, and 690 as intermediate–flux (IF) states, and orbit 181 as the high–flux (HF) state of 1H 0419–577 (see Pounds et al 2004b for a slightly different grouping of the observations).

The XMM–Newton observations of 1H 0419–577 reveal a clear trend with flux: as shown by Pounds et al (2004b) the hard 2–10 keV spectral index steepens, while the soft excess is more gradual as the X–ray flux increases. As an example, in Fig. 4, we show the ratio to a power–law model fitted between 2 and 10 keV only for two observations which are taken as representative of a low–flux (orbit 558) and high–flux (orbit 181) state. In the low–flux state, the 2–10 keV spectrum is very hard with $\Gamma = 1.31 \pm 0.06$, and a steep soft excess appears below about 0.8 keV. On the other hand, in the high–flux state, the hard spectrum is much steeper with $\Gamma = 1.80 \pm 0.05$, and the soft excess is already present at 1.5 keV and steepens at low energy much more gradually. In the top panel

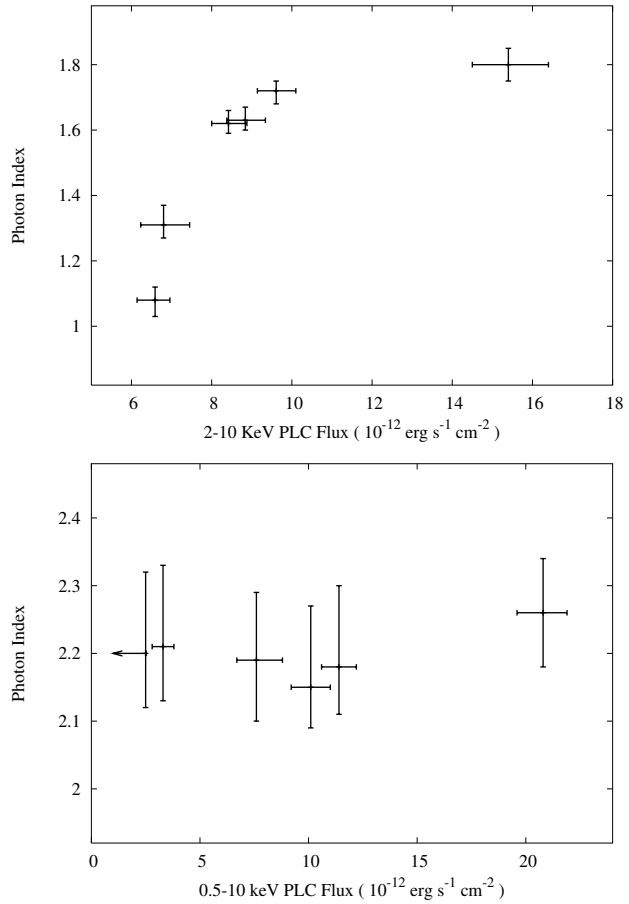

Figure 5. Top: The 2-10 keV photon index as a function of the PLC flux in the same band. The data have been fitted with a simple power law model. **Bottom**: The photon index from our best–fit model comprising a PLC and a RDC from the accretion disc as a function of the PLC flux. Once the RDC is properly considered, the photon index appears to be consistent with a constant (with $\Gamma \simeq 2.2$).

of Fig. 5, we plot the 2–10 keV photon index as a function of the 2–10 keV PLC flux, showing the gradual steepening of the hard spectrum with flux. The fitted spectral model only comprises the PLC. The same behaviour is found in other sources (e.g. MCG–6-30-15, see Shih et al 2002) and can often be understood in terms of a constant-Γ PLC which varies in normalisation affected by a weakly variable RDC. Given that the correlation of the 2–10 keV photon index and of the soft excess shape with flux is confirmed for all the observations, we believe that the X-ray variability of 1H 0419–577 should be explained by a model that *simultaneously* accounts for both correlations.

Any constant (or weakly variable) soft emission component would explain the spectral shape behaviour of the soft excess with flux which would be the result of the superposition of a constant soft emission and a variable power law component. Indeed, the soft emission in 1H 0419–577 is weakly variable as demonstrated by the analysis of the difference spectra by Pounds et al (2004b). One remarkable result of their analysis is that, while all the individual spectra do exhibit soft excesses, none of the difference spectra does, showing the constancy (or reduced variability) of the soft emission component in 1H 0419–577. One possibility put forward is provided by emission from photoionised circumnuclear gas. Given that emission from such a gas is observed in other sources (mainly Seyfert 2 nuclei in which the gas emission is not diluted into the primary continuum) this is certainly an attractive scenario which however does not provide a clear and simultaneous explanation for the 2-10 keV photon index correlation with flux.

An alternative can be given in terms of the two–component (RDC plus PLC) model in which the RDC varies little while a PLC with constant Γ and variable normalisation determines the flux state of the source. In such a model, the constant soft excess is due to a soft RDC spectrum which dominates the PLC in the LF states and is more and more contaminated by it as the flux increases, reproducing the soft spectral shape–flux observed correlation. On the other hand, the RDC gives rise to a very flat 2–10 keV spectrum in the LF and reflection–dominated states, while as the flux increases and the PLC overwhelms the RDC in the hard band, the spectrum steepens approaching asymptotically the PLC spectral shape. This simple idea can be visualised by considering a constant RDC and variable PLC in Fig. 3 and provides a natural, though not unique, simultaneous explanation for the soft excess spectral shape and photon index behaviour with the source flux. We point out here that a weakly variable RDC despite large amplitude PLC variability is precisely the behaviour induced by the light bending model (Miniutti & Fabian 2004).

4.1 Spectral analysis

In the following, we adopt the composite–reflection model that successfully explains the LF state of orbit 512 (Section 3) and apply it to the remaining XMM–Newton observations. The iron abundance, inner/outer disc radii, and disc inclination are fixed to the best–fit values found fitting orbit 512 data. All observations are extremely well fitted by the model, with reduced χ^2 very close to unity. The most relevant parameters and the resulting statistics are given in Table 2 for all observations. We do not report the parameters of the relativistic blurring which are similar to those already reported for the LF state of orbit 512 (see Section 3), with a very steep emissivity in the inner disc flattening in the outer regions and a break radius around $4\ r_g$. The HF state of orbit 181 exhibits a slightly flatter emissivity. In the framework of our model, HF states correspond to situations in which the primary PLC source is located at larger distance from the black hole than in LF states. Therefore, light bending is less effective, the disc illumination is much more uniform, and the resulting emissivity is indeed expected to be flatter.

The first interesting result is the photon index behaviour with flux. Once the RDC is properly taken into account, the behaviour shown in Fig. 5 (top panel) disappears, and the measured photon index is consistent with a constant as shown in the bottom panel of Fig. 5 and Table 2. A value of $\Gamma \simeq 2.2$ is consistent with the observed photon index at all flux levels, showing that the spectral variability is not dominated by a variable spectral slope of the primary X–ray continuum.

As pointed out by Pounds et al (2004b), a variable absorption component local to the source is also present. We have parametrised it with a phenomenological model comprising cold redshifted absorption and edge roughly reproducing the presence of a warm absorber. If our phenomenological (and rather crude) model for the warm absorber is replaced with more sophisticated descriptions such as that provided by the `ABSORI` model in `XSPEC` (Done et al 1992; Zdziarski et al. 1995) with Fe abundance tied to the reflector one, no significant differences in χ^2 is seen in any of the observations. Given the quality of the data, our phenomenological description seems sufficient to catch the main features of the absorber and,

XMM orbit	181 (HF)	512 (LF)	558 (LF)	605 (IF)	649 (IF)	690 (IF)
Γ	2.26 ± 0.08	$2.20^{+0.12}_{-0.08}$	$2.21^{+0.12}_{-0.08}$	$2.18^{+0.12}_{-0.07}$	$2.15^{+0.12}_{-0.06}$	$2.19^{+0.10}_{-0.09}$
$F_{\rm PLC}$	$20.8^{+1.1}_{-1.2}$	< 2.5	3.3 ± 0.5	11.4 ± 0.8	10.1 ± 0.9	$7.6^{+1.2}_{-0.9}$
$\xi_{\rm in}$	75 ± 15	69 ± 20	68 ± 18	56 ± 23	56 ± 21	61 ± 21
$\xi_{\rm out}$	38 ± 16	29 ± 16	29 ± 13	13^{+14}_{-6}	12^{+18}_{-8}	11^{+16}_{-4}
$F_{\rm RDC}$	$10.1^{+2.5}_{-2.4}$	$9.4^{+5.0}_{-2.7}$	$7.1^{+3.3}_{-1.9}$	$6.1^{+1.2}_{-1.3}$	$5.5^{+2.9}_{-1.7}$	$6.4^{+3.7}_{-1.6}$
χ^2/dof	605/614	620/637	621/631	762/800	803/764	724/755

Table 2. Results from the spectral fits to the six XMM–Newton observations with the composite two–component model. The 0.5–10 keV unabsorbed fluxes are given in units of 10^{-12} erg cm^{-2} s^{-1}, and the ionisation parameters in erg cm s^{-1}.

most importantly, does not affect our results on the RDC and PLC parameters which are our main interest here. The edge is present in all cases with energy around $0.74 - 0.78$ keV but its depth clearly diminishes with increasing flux. The absorbing column also drops as the flux increases from about 10^{21} cm^{-2} to zero, showing that absorption is more important in low than high flux states. However, the analysis of the difference spectra performed by Pounds et al (2004b) clearly shows that absorption is certainly important in this source (with signatures mainly from O, Fe, and Ne in the 0.5-1 keV band) but is not the main driver of the variability which is instead dominated by a steep power law component.

Our modelling allows us to identify the variable component with the PLC providing the X–ray continuum and illuminating the accretion disc where it is reprocessed and converted into the RDC. As mentioned, the PLC is consistent with having constant spectral shape and only its normalisation appears to vary. The variation of the PLC normalisation is at least a factor 9 between the LF and HF states and determines the flux state of 1H 0419–577 (see Table 2).

On the other hand, the RDC varies with a much smaller amplitude (about a factor 2), and is almost consistent with being constant within the errors at all flux levels (see Table 2). In Fig. 6, we show the unabsorbed best–fit RDC and PLC models for a LF (orbit 558, dotted grey) and for the HF (orbit 181, solid black) observation. The PLC variation is about a factor 7, while the RDC is consistent with being constant within the 90 per cent errors despite the very different flux state. This clarifies the reason why no soft excess is measured in difference spectra obtained between the various flux states (Pounds et al 2004b).

Since the RDC varies much less than the PLC, as the PLC flux drops the spectrum becomes more and more reflection–dominated, as expected if the light bending model applies at least qualitatively in this source. This can be shown by plotting the reflection fraction as a function of the PLC flux for the six observations. As a measure of the reflection fraction, i.e. of the RDC flux relative to the PLC continuum, we consider the $F_{\rm RDC}$ to $F_{\rm PLC}$ ratio in the whole 0.5–10 keV observable energy band. The resulting behaviour with the PLC is shown in Fig. 7 where the anti–correlation is clearly seen. The anti–correlation of the relative contribution of the RDC to the total flux is one of the distinctive characteristic of the light bending model proposed by Miniutti & Fabian 2004 to explain the spectral variability of X–ray sources in which a relativistic reflection component is observed (e.g. MCG–6-30-15, 1H 0707–495, the Galactic black hole candidate XTE J1650–500), making 1H 0419–577 one additional candidate for observing the effects of strong gravity in the immediate vicinity of an accreting black hole via X–ray observations.

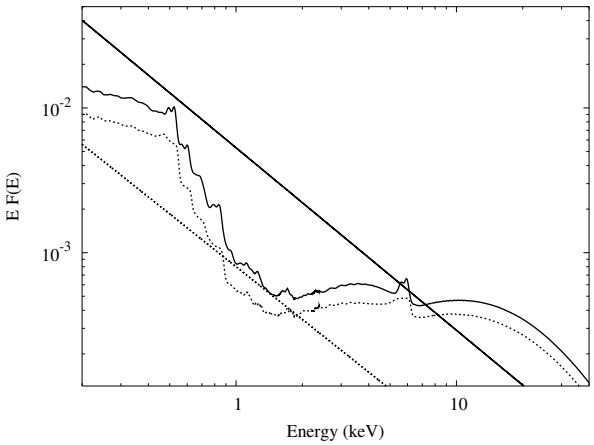

Figure 6. The unabsorbed best–fit RDC and PLC models for a LF state observation (orbit 558, dotted grey) and a HF state one (orbit 181, solid black). The PLC variation is about a factor 7, while the RDC is consistent with being constant within the errors (see Table 2). This is the reason why no (or very little) soft excess is seen in difference spectra between the various spectral states (Pounds et al 2004b).

The observed 0.5–10 keV X–ray luminosity of the source varies from 2×10^{44} erg/s (low state) to 8.3×10^{44} erg/s (high state), which is in the range of about 1–4 per cent of the bolometric (2.4×10^{46} erg/s, Grupe et al. 2004). In the framework of our model, the intrinsic PLC luminosity is constant (or varies little) and it is mostly light bending that induces the observed variations. The intrinsic PLC luminosity can then be estimated e.g. from the high–state (orbit 181), in which the PLC contribution to the 0.5–10 keV flux is about twice as large as the RDC (see Table 2 and Fig. 7), and turns out to be of the order of 10–20 per cent of the bolometric.

5 DISCUSSION

We have analysed all six available XMM–Newton EPIC–pn observations of 1H 0419–577. The source was observed in widely different flux states, allowing us to group the observations in low flux (LF), intermediate flux (IF) and high flux (HF) states and to study the spectral variability. 1H 0419–577 exhibits a strong soft excess at all flux levels, but steeper in the LF states and more gradual in the HF states. On the other hand, the hard 2–10 keV spectrum, when modelled with a simple power law, is clearly correlated with flux. In the LF state, the 2–10 keV photon index is implausibly hard (about

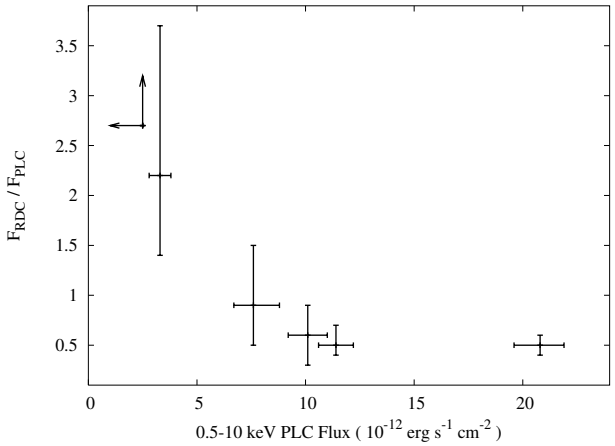

Figure 7. The ratio between the 0.5–10 keV flux of the RDC to the PLC is shown as a function of the PLC flux. This is a measure of the reflection fraction, i.e., the relative contribution of the RDC to the total flux. The observed anti–correlation is in very good agreement with the predictions of the light bending model (Miniutti & Fabian 2004).

1–1.3) for Comptonisation models, while it seems to saturate above 1.8 in the HF state.

We apply a two–component model to all observations comprising a PLC and a RDC from the accretion disc, modified by absorption (both Galactic and local to the source). We find that the spectral variability of 1H 0419–577 can be described by a strongly variable PLC with constant spectral shape ($\Gamma \simeq 2.2$ at all flux levels) and an almost constant ionised RDC. The photon index is therefore found to be much more consistent with the values allowed by standard Comptonisation models, and the spectral variability does not appear to be driven by photon index variations.

The RDC is affected by strong relativistic effects suggesting that it originates in the innermost regions of the accretion disc around a rapidly rotating Kerr black hole. The RDC is responsible for the soft excess and its weak variability explains the lack of any soft excess in the difference spectra between the various flux states, as shown in previous analysis (Pounds et al 2004b). The difference spectra show indeed that the variability is dominated by a steep power law which can be identified with the PLC of our spectral decomposition.

A major consequence of the above variability is that the spectrum becomes more and more reflection–dominated as the flux drops. Indeed, our analysis reveals that the spectrum of the lowest flux observation (orbit 512) can be interpreted as almost completely reflection–dominated. The RDC simultaneously explains both the soft excess, the flat 2–10 keV spectral shape, and the broad residuals in the Fe K band during the LF state. The parameters of the relativistic blurring and the behaviour of the reflection fraction with flux match the prediction of our light bending model, in which the primary source of the PLC is located in the region of strong gravity within a few gravitational radii from the central black hole.

Given the quality of the present data, the model we are proposing is not unique and other interpretations of the X–ray spectrum and variability of 1H 0419–577 are possible. Pounds et al (2004a; 2004b) consider as preferential a model in which the soft emission comprises an almost constant "core" component due to emission from photoionised gas, while the soft excess is entirely an artifact of absorption by a warm absorber. We point out that observing soft X–ray emission by photoionised gas would be somewhat unusual in such a high luminosity source. On the other hand, the flat photon index of the low flux state is explained by Pounds et al with the presence of a substantial column of additional cold matter that covers only partially the source and produces an absorption edge and spectral curvature in the Fe K band.

Our spectral decomposition has the great advantage of explaining the broadband spectrum and variability with the interplay of only two (broadband) components without the need of invoking separate components in the different energy bands. In addition it provides a natural explanation for the remarkably uniform temperature of 100–200 eV found in the soft X–ray spectra of a large number of low redshift active galaxies with soft excess (Gierlinski & Done 2004, Porquet et al 2004) despite large differences in black hole mass and luminosity (hence in accretion disc temperatures). The very narrow range of temperatures might indicate an origin in atomic (rather than truly thermal) processes for the soft excess. Absorption, as proposed by Pounds et al (2004b) for 1H 0419–577, provides a possibility, but some active galaxies exhibit a soft excess despite the lack of any absorption signature (see e.g. Ark 120, Vaughan et al 2004). The other natural explanation involves relativistically blurred ionised reflection (and bremsstrahlung from the disc surface layers). The ionised reflection model we are using is indeed well fitted by a 100–200 eV blackbody for a wide range of ionisation and blurring parameters, when folded through the EPIC–pn response matrix in the 0.3-2 keV band (Ross & Fabian 2005).

We note that the small inner disc radius required by our model, with $r_{\rm in} \leqslant 2\,r_g$ in the lowest flux state, and the relatively low ionisation of the disc material, indicate that high density gas extends down to those radii. Although magnetic field and mass accretion rate nonaxisymmetric variations can distort the inner reflecting radius of a disc (Krolik & Hawley 2002), we doubt that the innermost stable circular orbit (ISCO) can be much further out than $2\,r_g$. Since the ISCO is related to the spin parameter a of the black hole by a simple formula (see e.g. Bardeen, Press & Teukolsky 1972), the upper limit on $r_{\rm in}$ translates into a lower limit for the black hole spin parameter in 1H 0419–577 of $a \geqslant 0.95$.

A much longer XMM–Newton exposure of 1H 0419–577 during a low flux state would help resolving the partial covering/broad iron line degeneracy. Moreover, the forthcoming launch of the Astro–E2 X–ray satellite, with unprecedented energy resolution in the Fe K band, could help resolving this issue in 1H 0419–577 and other sources. If the edge detected at 7.1 keV is due to absorption, it will be reasonably sharper than if it is due to the combination of a reflection edge and the blue wing of a relativistic line, the difference between the two models being within the grasp of the Astro–E2 capabilities. The 2–10 keV luminosity of 1H 0419–577 makes this source a potential important target for Astro–E2, as opposed to 1H 0707-495 which is about one order of magnitude fainter in the 5–7 keV band.

ACKNOWLEDGMENTS

Based on observations obtained with XMM-Newton, an ESA science mission with instruments and contributions directly funded by ESA Member States and NASA. We also thank Ken Pounds for kindly providing the data that were used in this work. ACF thanks the Royal Society for support. GM and KI thank the PPARC, and RRR the College of the Holy Cross for support.

REFERENCES

Bardeen J.M., Press W.H., Teukolsky S.A., 1972, ApJ, 178, 347
Done C., Mulchaey J.S., Mushotzky R.F., Arnaud K.A., 1992, ApJ, 395, 275
Fabian A.C., Ballantyne D.R., Merloni A., Vaughan S., Iwasawa K., Boller T., 2002, MNRAS, 331, 35
Fabian A.C., Vaughan S., 2003, MNRAS, 340, L28
Fabian A.C., Miniutti G., Gallo L., Boller Th., Tanaka Y., Vaughan S., Ross R.R., 2004, MNRAS, 353, 1071
Ghisellini G., Haardt F., Matt G., 2004, A&A, 413, 535
Gierlinski M., Done C., 2004, MNRAS, 349, L7
Guainazzi M. et al, 1998, A&A, 339, 327
Grupe D., Wills B.J., Leighly K.M., Meusinger H., 2004, AJ, 127, 156
Haardt F., Maraschi L., 1991, ApJ, 380, L51
Iwasawa K., Miniutti G., Fabian A.C., 2004, MNRAS, 355, 1073
Kaspi S., Smith P.S., Netzer H., Maoz D., Jannuzi B.T., Giveon U., 2000, ApJ, 533, 631
Kirsch M.G.F. et al, 2004, (astro-ph/0407257)
Krolik J.H., Hawley J.F., 2002, ApJ, 573, 754
Laor A., 1991, ApJ, 376, 90
Markoff S., Falcke H., Fender R., 2001, A&A, 372, L25
Marshall H.L., Fruscione A., Carone T.E., 1995, ApJ, 439, 90
Martocchia A., Karas V., Matt G., 2000, MNRAS, 312, 817
Miniutti G., Fabian A.C., Goyder R., Lasenby A.N., 2003, MNRAS, 344, L22
Miniutti G., Fabian A.C., 2004, MNRAS, 349, 1435
Miniutti G., Fabian A.C., Miller J.M., 2004, MNRAS, 351, 466
Page K.L., Pounds K.A., Reeves J.N., O'Brien P.T., 2002, MNRAS, 330, L1
Porquet D., Reeves J.N., O'Brien P., Brinkmann W., 2004, A&A, 422, 85
Pounds K.A., Reeves J.N., Page K.L., O'Brien P.T., 2004a, ApJ, 605, 670
Pounds K.A., Reeves J.N., Page K.L., O'Brien P.T., 2004b, ApJ, 616, 696
Pye J.P. et al, 1995, MNRAS, 274, 1165
Ross R.R., Fabian A.C., 1993, MNRAS, 261, 74
Ross R.R., Fabian A.C., Young A.J., 1999, MNRAS, 306, 461
Ross R.R., Fabian A.C., Ballantyne D.R., 2002, MNRAS, 336, 315
Ross R.R., Fabian A.C., 2005, MNRAS in press, (astro-ph/0501116)
Rossi S., Homan J, Miller J.M., Belloni T., 2005, MNRAS in press (preprint astro-ph/0504182)
Shemmer O., Netzer H., Maiolino R., Oliva E., Croom S., Corbett E., di Fabrizio L., 2004, ApJ, 614, 547
Shih D.C., Iwasawa K. Fabian A.C., 2002, MNRAS, 333, 687
Turner T.J. et al, 1999, ApJ, 510, 178
Vaughan S., Fabian A.C., 2004, MNRAS, 348, 1415
Vaughan S., Fabian A.C., Ballantyne D.R., de Rosa A., Piro L., Matt G., 2004, MNRAS, 351, 193
Zdziarski A.A., Johnson W.N., Done C., Smith D., McNaron-Brown K., 1995, ApJ, 438, L63